

## ORIGINAL ARTICLE

# Protection against neonatal respiratory viral infection via maternal treatment during pregnancy with the benign immune training agent OM-85

Jean-Francois Lauzon-Joset<sup>1,2†</sup>, Kyle T Mincham<sup>2†</sup>, Naomi M Scott<sup>2</sup>, Yasmine Khandan<sup>2</sup>, Philip A Stumbles<sup>2,3</sup>, Patrick G Holt<sup>2</sup> & Deborah H Strickland<sup>2</sup>

<sup>1</sup>Centre de Recherche, Institut Universitaire de Cardiologie et de Pneumologie de Québec, Université Laval, Québec, QC, Canada

<sup>2</sup>Telethon Kids Institute, University of Western Australia, Nedlands, WA, Australia

<sup>3</sup>Medical, Molecular and Forensic Sciences, Murdoch University, Perth, WA, Australia

## Correspondence

Deborah H Strickland, Telethon Kids Institute, University of Western Australia, Nedlands, WA, Australia.  
E-mail: Deb.Strickland@telethonkids.org.au

<sup>†</sup>Co-first author.

Received 15 March 2021;

Revised 20 May and 2 June 2021;

Accepted 2 June 2021

doi: 10.1002/cti2.1303

*Clinical & Translational Immunology*  
2021; 10: e1303

## Abstract

**Objectives.** Incomplete maturation of immune regulatory functions at birth is antecedent to the heightened risk for severe respiratory infections during infancy. Our forerunner animal model studies demonstrated that maternal treatment with the microbial-derived immune training agent OM-85 during pregnancy promotes accelerated postnatal maturation of mechanisms that regulate inflammatory processes in the offspring airways. Here, we aimed to provide proof of concept for a novel solution to reduce the burden and potential long-term sequelae of severe early-life respiratory viral infection through maternal oral treatment during pregnancy with OM-85, already in widespread human clinical use. **Methods.** In this study, we performed flow cytometry and targeted gene expression (RT-qPCR) analysis on lungs from neonatal offspring whose mothers received oral OM-85 treatment during pregnancy. We next determined whether neonatal offspring from OM-85 treated mothers demonstrate enhanced protection against lethal lower respiratory infection with mouse-adapted rhinovirus (vMC<sub>0</sub>), and associated lung immune changes. **Results.** Offspring from mothers treated with OM-85 during pregnancy display accelerated postnatal seeding of lung myeloid populations demonstrating upregulation of function-associated markers. Offspring from OM-85 mothers additionally exhibit enhanced expression of TLR4/7 and the IL-1 $\beta$ /NLRP3 inflammasome complex within the lung. These treatment effects were associated with enhanced capacity to clear an otherwise lethal respiratory viral infection during the neonatal period, with concomitant regulation of viral-induced IFN response intensity. **Conclusion.** These results demonstrate that maternal OM-85 treatment protects offspring against lethal neonatal respiratory viral infection by accelerating development of innate immune mechanisms crucial for maintenance of local immune homeostasis in the face of pathogen challenge.

**Keywords:** early-life infection severity, immune modulation, lung, OM-85, pregnancy, rhinovirus

## INTRODUCTION

Acute lower respiratory infections (LRIs) represent the leading cause of mortality among children younger than 5 years, accounting for more than 15% of all deaths in this age group.<sup>1</sup> When compared to the approximate 4.4% of deaths in people of all ages attributable to LRIs each year,<sup>2</sup> the urgent requirement for novel treatment strategies to protect specifically against the life-threatening effects of early postnatal respiratory infections becomes immediately apparent. Further reinforcing this need, less severe grades of LRI during infancy are also recognised as a major risk factor for subsequent early-onset asthma diagnosis, which contributes to a significant global health and economic burden impacting over 300 million individuals.<sup>3–5</sup>

Within both humans and experimental murine models, the classical pathophysiology of an innate antiviral response within the airways is characterised by the rapid influx of inflammatory neutrophils into the lungs, initially from the intrapulmonary endothelial marginating pool and subsequently from the bone marrow via the circulating pool,<sup>6–8</sup> with concurrent secretion of uniquely high levels of type I interferon (IFN)- $\beta$  and type II IFN- $\gamma$ , primarily by plasmacytoid dendritic cells (pDC) and natural killer (NK) cells respectively.<sup>9,10</sup> Human studies indicate that persistent activation of these innate pathogen response pathways and aberrant/dysregulated production of inflammatory cytokines can lead to collateral tissue damage within the lungs and subsequent chronic lung pathology or death.<sup>11–13</sup> This unregulated inflammatory response is exaggerated in infants with acute viral bronchiolitis, whereby those presenting with severe symptoms, including febrile episodes, display hyperactivation of IFN-associated gene networks within both whole blood/peripheral blood mononuclear cells and the nasal mucosa.<sup>14,15</sup> As such, therapeutic interventions capable of maintaining the delicate balance between appropriate antiviral immunity and limitation of destructive pathology would provide a means to mitigate unnecessary viral-induced comorbidities.

However, there are major challenges associated with protecting the highly vulnerable neonatal/

infant age group against infectious disease mortality. For one, infant responsiveness to immune-enhancing therapeutics, including conventional vaccination, is constrained to variable degrees by development-associated deficiencies in innate and adaptive immune functions that mature postnatally, exemplified by the interleukin (IL)-1 $\beta$ -NOD-like receptor family pyrin domain containing 3 (NLRP3) inflammasome complex,<sup>16,17</sup> expression of Toll-like receptor (TLR)<sup>18</sup> microbial sensing machinery and competence of mucosal dendritic cell (DC) networks.<sup>19–23</sup> In the present study, we have examined the novel hypothesis that pre-programming key aspects of the aforementioned innate immune functions before birth via delivering beneficial innate immune training signals to the foetus will provide a mechanism to circumvent early developmental immune deficiencies, potentially mitigating the risk of death following severe early-life LRI.<sup>24</sup> This approach is based on our forerunner studies with the microbial-derived immune training agent OM-85, which has been in widespread clinical use for more than 30 years for limiting the risk of severe respiratory infections in young children from preschool age.<sup>24–28</sup> Our previous studies have shown that OM-85 treatment of pregnant mice markedly enhanced resistance to the pregnancy-threatening effects of exposure to bacterial and viral pathogens, which was associated with the modulation of myeloid cell recruitment/egression within inflamed gestational tissues.<sup>29</sup> Moreover, OM-85 treatment of pregnant mice was also shown to promote maturation of foetal bone marrow myeloid progenitor populations, resulting in accelerated postnatal establishment of functionally mature dendritic cell (DC) networks in the respiratory mucosal tissues of their offspring. This was accompanied by enhanced capacity of regulatory T cells (Treg) to regulate the intensity/duration of allergic airway inflammatory responses.<sup>30,31</sup> Given that similar DC/Treg-associated mechanisms are central to protection against infection-induced inflammatory tissue damage in the lower respiratory tract, we posited that maternal OM-85 treatment could also enhance resistance to a lethal viral LRI in the offspring during the highly vulnerable neonatal

period, and testing this hypothesis was the focus of the experiments reported below. Neonatal offspring from mothers treated with oral OM-85 during pregnancy were infected with a mouse-adapted rhinovirus (vMC<sub>0</sub>) at 2 days of age, and the clinical, cellular and targeted gene expression response within the neonatal lungs was evaluated during the acute, peak and resolution phases of infection.

## RESULTS

### Accelerated postnatal development of the myeloid compartment within neonatal lungs following maternal OM-85 treatment

Given our previous findings of enhanced myelopoiesis in foetal bone marrow following OM-85 treatment of pregnant mice,<sup>30</sup> we first sought to determine the influence of maternal OM-85 treatment on baseline postnatal development of immune cell populations in the lungs of their offspring. Time-mated pregnant mice were orally treated with OM-85 from gestation day (GD) 0.5–17.5, followed by natural term delivery of offspring 2–3 days later ( $\approx$ GD20.5). Offspring lungs were collected and analysed using multicolour flow cytometry (gating strategies shown in Supplementary figure 1) at postnatal days (PND) 3, 7, 12 and 22. As shown in Figure 1, the most profound treatment effects were observed during the neonatal/early infancy period (PND 3–7), including accelerated accumulation of plasmacytoid DC (pDC; Figure 1a), macrophage subsets (Figure 1b, c) and monocytes (Figure 1d). We further observed OM-85-induced changes in conventional DC (cDC) 1 and cDC2 populations, with a significant increase in the proportion of both subsets at PND 12 and upregulation of the function-associated molecules MHC class II (I-A/I-E) and CD86 at PND 3–7 (Figure 1e–j). These OM-85 treatment-associated changes in myeloid cell populations were accompanied by an increase in myeloid-derived suppressor cells (MDSC; Figure 1k), which have previously been shown to play a key role in controlling inflammation in neonatal humans and mice<sup>32</sup>, and also enhanced accumulation of Treg (Figure 1l) and cells expressing a phenotype resembling that of type 2 innate lymphoid cells (ILC2; data not shown) at PND 7. Collectively, these findings are consistent with maternal OM-85

treatment transplacentally inducing an enhanced rate of postnatal respiratory myeloid cell maturation in the offspring, with the potential for increased capacity to maintain respiratory immunological homeostasis in the face of proinflammatory challenges during the early postnatal period.

### Maternal OM-85 treatment upregulates TLR4 and TLR7 expression in offspring lungs

To further characterise the underlying mechanism (s) of action of maternal OM-85-driven transplacental innate immune enhancement, we measured early postnatal gene expression of a range of immunoregulatory cytokines, cellular sensors and key signatures associated with innate immune training within peripheral lungs of offspring from OM-85-treated mothers. Maternal OM-85 treatment resulted in accelerated postnatal upregulation of both *IL-1 $\alpha$*  and *IL-1 $\beta$*  (key immune training signature) gene expression, which reached statistical significance by PND 22 (Figure 2a, b). This mirrors prior observations in independent model systems following OM-85 treatment of murine macrophages.<sup>33</sup> Given the dependency of *IL-1 $\beta$*  production on *NLRP3* and *caspase-1*, and the functional deficiency in this pathway during prenatal and early neonatal life,<sup>16,17</sup> we next assessed the impact of maternal OM-85 treatment on gene expression levels of these upstream targets in offspring lungs. As demonstrated in Figure 2c, maternal OM-85 treatment upregulated *NLRP3* expression at all time points measured during the first 22 days of life in their offspring; however, downstream concomitant upregulation of *caspase-1* was only evident at PND 22 (Figure 2d), corresponding to the observed upregulation of *IL-1 $\alpha/\beta$*  expression. Lastly, there is now compelling evidence in both humans<sup>34–36</sup> and experimental murine models<sup>37</sup> demonstrating that the immunomodulatory effects of beneficial microbial exposures, including those of OM-85,<sup>38</sup> are mediated via the enhanced baseline expression of TLRs. We therefore assessed the expression levels of *TLR4* and *TLR7* within neonatal peripheral lungs, with both receptors significantly upregulated across all early postnatal time points within offspring from OM-85-treated mothers (Figure 2e, f), consistent with the centrality of this innate mechanism in immunomodulator-mediated transplacental immune training.

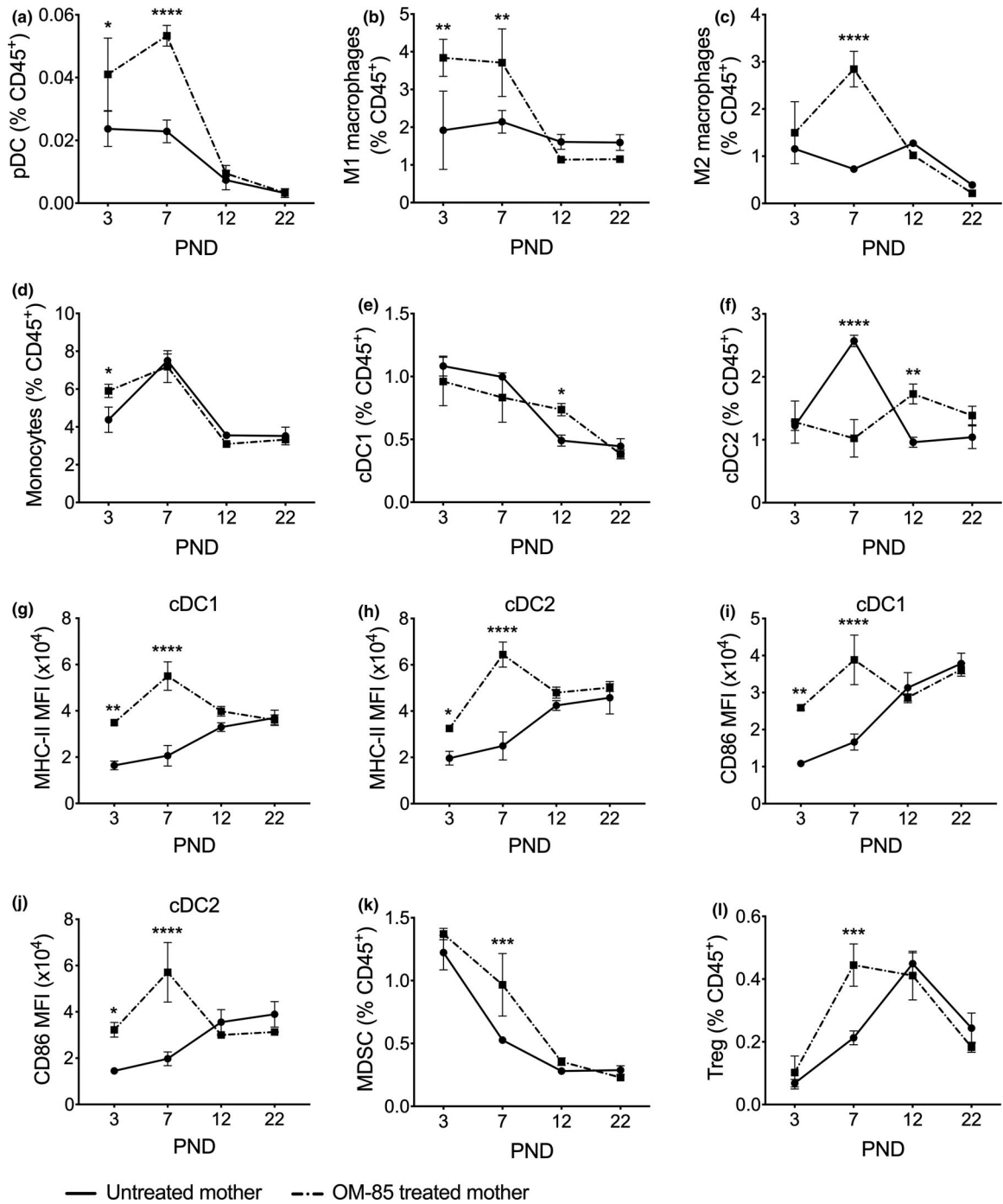


**Figure 1.** Maternal OM-85 treatment promotes myelopoiesis within neonatal lungs. **(a)** Plasmacytoid dendritic cells (pDC), **(b)** M1 macrophages, **(c)** M2 macrophages, **(d)** monocytes, **(e)** conventional DC (cDC) 1 and **(f)** cDC2 as a proportion of CD45<sup>+</sup> cells within neonatal peripheral lungs. **(g, h)** Mean fluorescence intensity (MFI) of I-A/I-E expression on **(g)** cDC1 and **(h)** cDC2 within neonatal peripheral lungs. **(i, j)** MFI of CD86 expression on **(i)** cDC1 and **(j)** cDC2 within neonatal peripheral lungs. **(k)** Myeloid-derived suppressor cells (MDSC) and **(l)** regulatory T cells (Treg) as a proportion of CD45<sup>+</sup> cells within neonatal peripheral lungs. Data are displayed as line plot showing mean ± SEM of *n* = 3–6 offspring from *n* = 3 independent experiments per group. Statistical significance was determined using the two-way ANOVA followed by the uncorrected Fisher's LSD test; \**P* < 0.05, \*\**P* < 0.01, \*\*\**P* < 0.001 and \*\*\*\**P* < 0.0001.

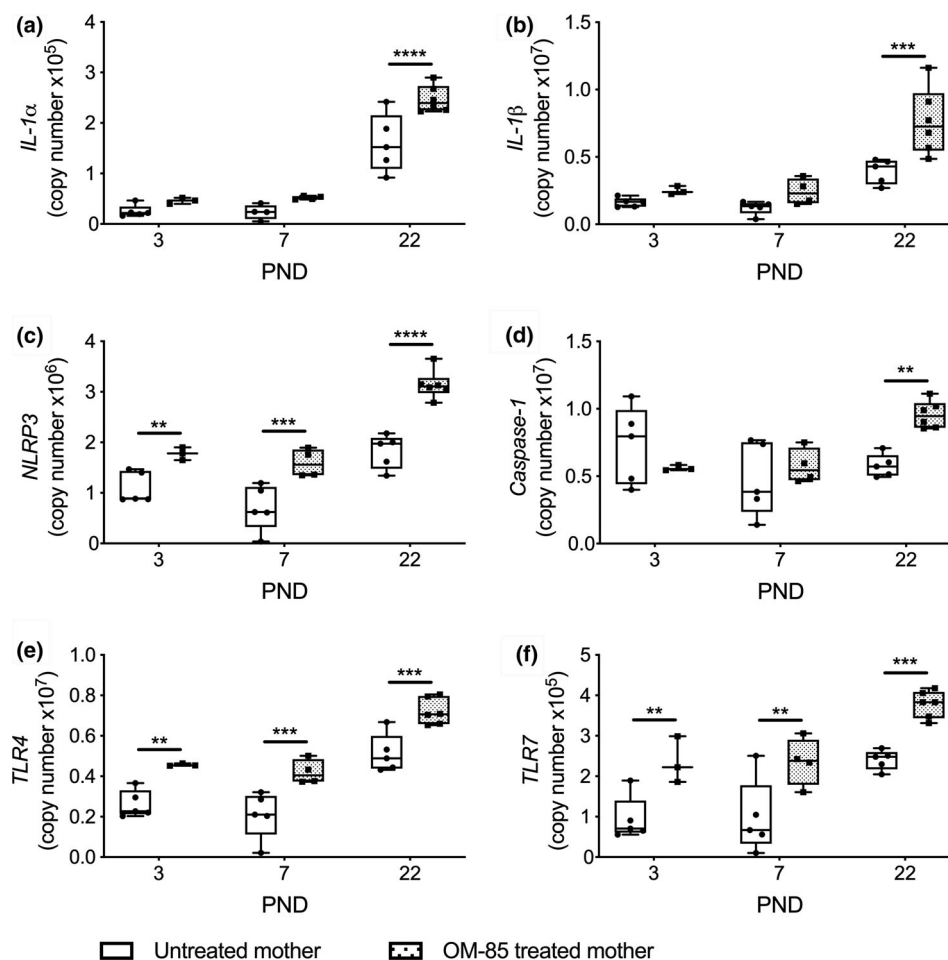


**Figure 2.** Maternal OM-85 treatment upregulates the  $IL-1\beta$  pathway and TLR expression in neonatal lungs. Absolute copy number of gene expression profiles for (a) *IL-1 $\alpha$* , (b) *IL-1 $\beta$* , (c) *NLRP3*, (d) *caspase-1*, (e) *TLR4* and (f) *TLR7* within the lungs of neonates from OM-85-treated and untreated mothers. Data are from individual mice and displayed as box-and-whisker plot showing minimum to maximum values of  $n = 3$ –6 offspring from  $n = 3$  independent experiments per gene. Statistical significance was determined using two-way ANOVA followed by uncorrected Fisher's LSD test; \*\* $P < 0.01$ , \*\*\* $P < 0.001$  and \*\*\*\* $P < 0.0001$ .

### Maternal OM-85 treatment protects neonates against vMC<sub>0</sub>-induced death

Having demonstrated that maternal OM-85 treatment enhanced postnatal establishment of respiratory immunocompetence, as defined by accelerated myelopoiesis and innate cytokine signalling pathways, we next sought to determine whether this would translate into enhanced protection against a lethal neonatal LRI. To address this, we developed a murine neonatal infection model of human rhinovirus (HRV), using live attenuated mengovirus (vMC<sub>0</sub>), a mouse-adapted mimic of HRV.<sup>7</sup> Given the age-dependent response observed in murine respiratory viral infection models,<sup>39–41</sup> our initial experiments aimed to determine the optimal vMC<sub>0</sub> dose required to

achieve 20–25% death (LD<sub>20–25</sub>) in PND 2 neonates. Neonatal offspring of untreated mothers were infected at PND 2 (henceforth referred to as day post-infection [DPI] 0) with a dose of  $10^3$ – $10^6$  plaque-forming units (PFU) of vMC<sub>0</sub>, and survival was assessed up to DPI 20 (Figure 3a). The typical experimental adult mouse LD<sub>20–25</sub> dose of  $10^6$  PFU<sup>7</sup> resulted in  $\approx 90\%$  death of infected PND 2 neonates by DPI 12 (Figure 3a). The LD<sub>20–25</sub> dose in neonates was achieved following infection with  $10^4$  PFU vMC<sub>0</sub>, and this dose was used for the remainder of the study (Figure 3a). We next sought to determine whether the severity of vMC<sub>0</sub>-induced clinical disease in neonates was modulated following OM-85 treatment of the pregnant mothers as described in Figure 3b. Maternal OM-85 treatment resulted in 100% protection against vMC<sub>0</sub>-induced neonatal

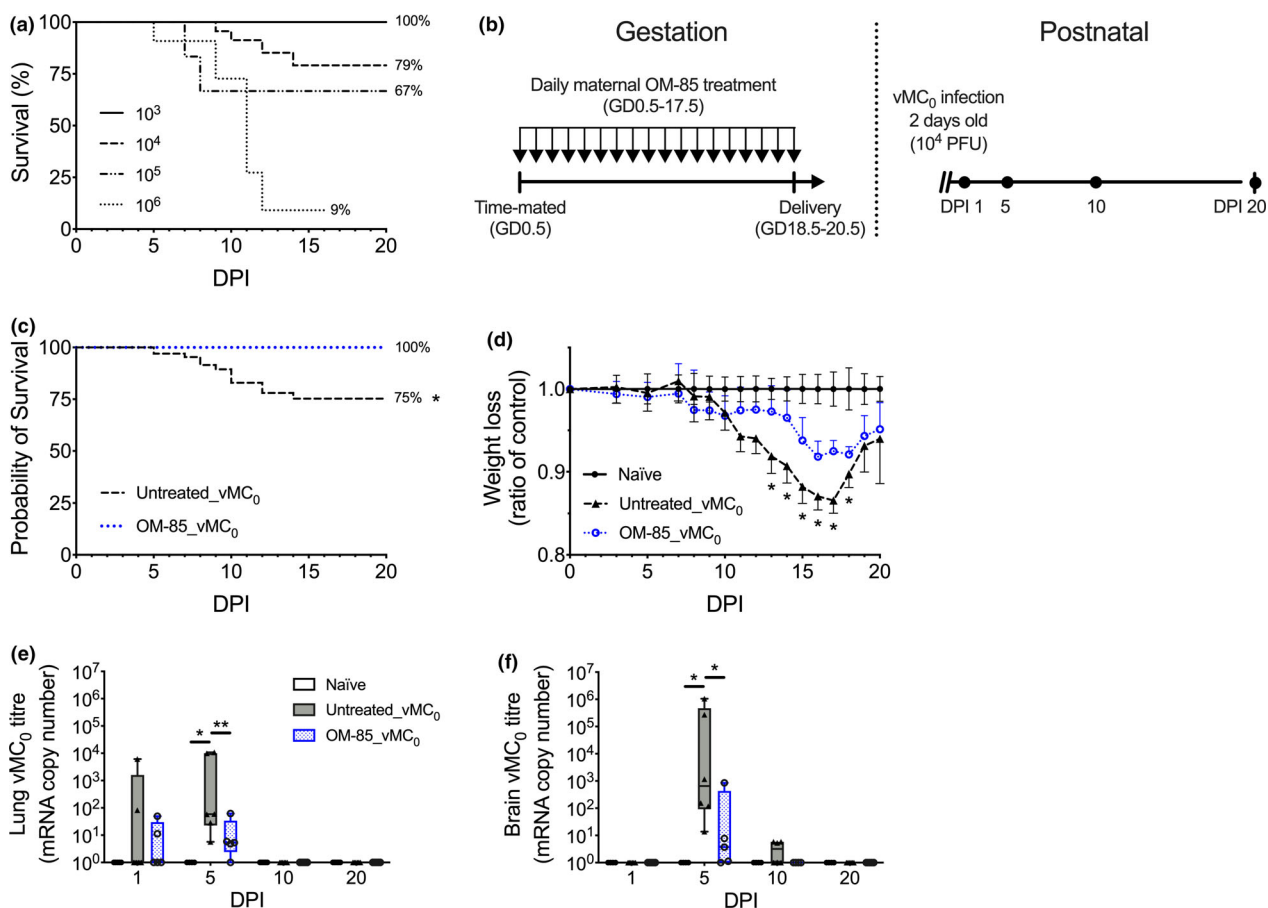


**Figure 3.** Maternal OM-85 treatment protects neonates against vMC<sub>0</sub> respiratory viral infection-induced death. **(a)** Titration of neonatal vMC<sub>0</sub> plaque-forming-units (PFU) required to achieve a lethal dose in 20–25% (LD<sub>20–25</sub>) of infected neonates ( $10^3$   $n = 12$ ,  $10^4$   $n = 38$ ,  $10^5$   $n = 6$  and  $10^6$   $n = 11$ ). Data are displayed as survival curves showing  $n = 12$  independent experiments. **(b)** Maternal OM-85 treatment regimen from gestation day (GD) 0.5–17.5 (left), followed by neonatal vMC<sub>0</sub> infection at 2 days of age and disease kinetics monitored until day post-infection (DPI) 20 (right). Neonates were autopsied and samples collected at DPI 1, 5, 10 and 20. **(c)** Survival curves of vMC<sub>0</sub>-infected neonates from OM-85-treated (OM-85\_vMC<sub>0</sub>;  $n = 19$ ) and untreated (Untreated\_vMC<sub>0</sub>;  $n = 33$ ) mothers. Data are displayed from  $n = 8$  independent experiments. Statistical significance was determined using the log-rank (Mantel–Cox) test and displayed as  $*P < 0.05$ . **(d)** Weight loss of vMC<sub>0</sub>-infected neonates from OM-85-treated and untreated mothers (naïve  $n = 28$ , untreated\_vMC<sub>0</sub>  $n = 33$ , OM-85\_vMC<sub>0</sub>  $n = 19$ ). Data are displayed as line plot showing mean  $\pm$  SEM of  $n = 12$  independent experiments. Statistical significance was determined using two-way ANOVA with Tukey's multiple comparisons test;  $*P < 0.05$  vs. control. **(e, f)** vMC<sub>0</sub> viral titres in the **(e)** lungs and **(f)** brain of neonates from OM-85-treated (OM-85\_vMC<sub>0</sub>) and untreated (Untreated\_vMC<sub>0</sub>) mothers. vMC<sub>0</sub> viral load of the control neonates was below the detection limit of the assay. Data are displayed as box-and-whisker plot showing minimum to maximum values of  $n = 4$ – $6$  offspring from  $n = 3$  independent experiments. Statistical significance was determined using two-way ANOVA followed by the uncorrected Fisher's LSD test;  $*P < 0.05$ .

death (Figure 3c) when compared to the offspring of non-treated mothers. Weight loss in vMC<sub>0</sub>-infected neonates was significantly less severe in those from OM-85-treated mothers compared with surviving infected neonates from untreated mothers (Figure 3d). Furthermore, maternal OM-85 treatment during pregnancy resulted in significantly reduced peak viral titres in both the lungs and brain of vMC<sub>0</sub>-infected neonates at the peak of infection compared with the offspring of untreated mothers (Figure 3e, f). This is consistent with our previous

findings demonstrating enhanced viral clearance in OM-85-treated versus untreated mothers<sup>29</sup> and independent studies in adult mice.<sup>42</sup>

### Attenuation of vMC<sub>0</sub>-induced innate proinflammatory cellular responses in neonatal lung tissue following maternal OM-85 treatment

In addition to the clinical assessments above, multiparameter flow cytometry was performed on

single-cell lung preparations to determine the impact of maternal OM-85 treatment on the cellular immune response to neonatal vMC<sub>0</sub> infection. Immunophenotypic characterisation of neonatal lungs revealed that the severity of the classical acute proinflammatory innate viral response was significantly attenuated in neonates from OM-85-treated mothers compared with equivalent neonates from untreated mothers. This included a reduced influx of neutrophils at DPI 1 (Figure 4a), natural killer (NK) cells at DPI 1 and DPI 5 (Figure 4b), and classical monocytes over the entire disease time course evaluated (Figure 4c). The early influx of pDC into the lungs of vMC<sub>0</sub>-infected neonates at DPI 1 (Figure 4d) was also dramatically less intense in offspring from OM-85-treated compared with untreated mothers; however, this pDC population exhibited a substantial increase in expression of MHC class II at the peak of viral load (Figure 4e), and also in CD40 expression during the ensuing resolution phase (Figure 4f). Immunophenotypic characterisation additionally identified multiple lung macrophage subsets in neonates; however, maternal OM-85 treatment had very little influence on these cell populations in vMC<sub>0</sub>-infected neonates compared with offspring of untreated mothers (Supplementary figure 2a–c). Together, these data indicate that maternal OM-85-mediated treatment effects induced a shift in the lung cellular immune response of the offspring following neonatal vMC<sub>0</sub> infection towards a state of improved homeostatic control and dampened inflammation within the lungs, while at the same time reducing viral load.

Within the lungs, cDC subsets represent a highly dynamic population that turn over rapidly, providing continuous signalling of incoming airborne antigens impacting respiratory surfaces to the T-cell system in lymph nodes and respiratory tissues.<sup>43,44</sup> In this regard, cDC1 are primarily responsible for the cross-presentation of viral antigen to CD8<sup>+</sup> T cells,<sup>43,45</sup> while their cDC2 counterparts are primarily involved in the generation of CD4<sup>+</sup> T-cell responses within regional airways draining lymph nodes. Following viral challenge of neonates from untreated mothers, we observed the specific modulation of both cDC subsets in neonatal lung tissue, including a significant reduction in cDC1 at DPI 1 (Figure 4g), while cDC2 proportions were reduced at the peak of infection at DPI 5 (Figure 4h), likely representing the complex interplay between

cellular efflux/influx within the bone marrow–lung–lymph node axis.<sup>46</sup> Of particular interest, vMC<sub>0</sub>-infected neonates from untreated mothers exhibited a deficit in cDC2 numbers, which persisted until infection resolution at DPI 20 (Figure 4h), consistent with previous findings that early-life influenza infection drives persistent dysregulation of local myeloid populations.<sup>47</sup> However, maternal OM-85 treatment was able to preserve lung cDC2 numbers at similar levels to those observed in age-matched non-infected controls (Fig 4h). Moreover, both cDC1 and cDC2 subpopulations displayed enhanced functional upregulation in the lungs of neonates from OM-85-treated mothers in response to vMC<sub>0</sub> challenge as evidenced by a significant increase in the function-associated molecules MHC class II (Figure 4i, j) and CD86 (Figure 4k, l) at peak viral load at DPI 5, although with no observable changes in CD40 expression (Supplementary figure 2d, e). Collectively, these observations are consistent with previous findings<sup>31</sup> indicating that maternal OM-85 treatment transplacentally regulates the foetal/neonatal bone marrow–lung axis towards development of lung myeloid cell regulatory networks more resilient to excessive inflammation in the face of early-life respiratory inflammation, through enhanced developmental trajectories of lung innate immune cell subsets that are crucial for maintenance of local immune homeostasis.

We also assessed T-cell responses in the lungs of vMC<sub>0</sub>-infected neonates from OM-85-treated and untreated mothers. At the peak of clinical disease (DPI 5), maternal OM-85 treatment induced a small but significant reduction in the frequency of CD8<sup>+</sup> T cells in the lungs of vMC<sub>0</sub>-infected offspring compared with equivalent offspring of untreated mothers (Figure 4m). Notably, while there was no significant influence of maternal OM-85 treatment on the overall CD4<sup>+</sup> T-cell pool in vMC<sub>0</sub>-infected neonates (Supplementary figure 2f), we identified an enhanced population of activated CD4<sup>+</sup> T cells at DPI 10 in infected neonates from OM-85-treated mothers (Figure 4n). These same neonates additionally displayed a significantly amplified pool of mucosal homing Treg within the peripheral lung from the peak of disease until resolution at DPI 20 (Figure 4o), while cells resembling a local ILC2 population were significantly upregulated from DPI 1–5 in vMC<sub>0</sub>-infected neonates from OM-85-treated neonates (data not shown). These findings

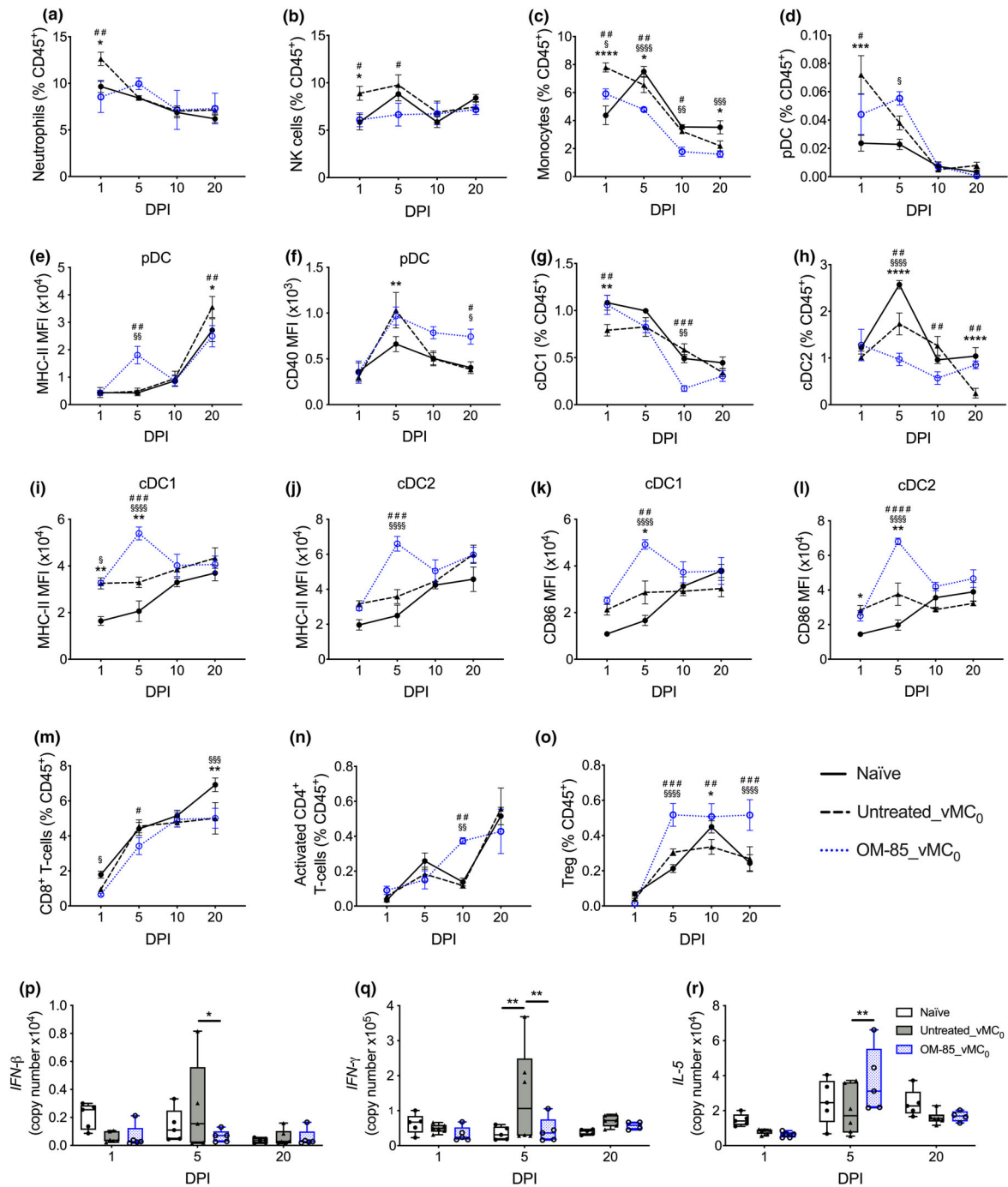


**Figure 4.** Maternal OM-85 treatment dampens the innate proinflammatory cellular response while enhancing regulatory responses within neonatal lungs following vMC<sub>0</sub> infection. **(a)** Neutrophils, **(b)** NK cells, **(c)** monocytes and **(d)** pDC as a proportion of CD45<sup>+</sup> cells within neonatal peripheral lungs. **(e, f)** MFI of **(e)** I-A/I-E and **(f)** CD40 expression on pDC. **(g)** cDC1 and **(h)** cDC2 as a proportion of CD45<sup>+</sup> cells. **(i, j)** MFI of I-A/I-E expression on **(i)** cDC1 and **(j)** cDC2. **(k, l)** MFI of CD86 expression on **(k)** cDC1 and **(l)** cDC2. **(m)** CD8<sup>+</sup> T cells and **(n)** activated CD4<sup>+</sup> T cells and **(o)** Treg as a proportion of CD45<sup>+</sup> cells. Data are displayed as line plot showing mean ± SEM of n = 4–6 offspring from n = 4 independent experiments per group. Statistical significance was determined using the two-way ANOVA followed by uncorrected Fisher’s LSD test; \*Naive vs. Untreated\_vMC<sub>0</sub>, \$Naive vs. OM-85\_vMC<sub>0</sub> and #Untreated\_vMC<sub>0</sub> vs. OM-85\_vMC<sub>0</sub>. **(p, r)** Absolute copy number of gene expression profiles for **(p)** *IFN-β*, **(q)** *IFN-γ* and **(r)** *IL-5* within neonatal peripheral lungs. Data are displayed as box-and-whisker plot showing minimum to maximum values of n = 4–6 offspring from n = 3 independent experiments per gene. Statistical significance was determined using two-way ANOVA followed by uncorrected Fisher’s LSD test, \*P < 0.05 and \*\*P < 0.01.

are consistent with our previous studies and those of others identifying Tregs as a crucial target for both the direct<sup>38,48</sup> and transplacental<sup>31</sup> protective effects of OM-85 treatment in inflammation-induced respiratory diseases during early life.

Finally, to gain further insight into the mechanisms promoting transplacental OM-85-mediated protection against vMC<sub>0</sub> infection severity in neonatal offspring post-birth, we measured the gene expression levels of key cytokines in neonatal lungs, including type I and type II IFNs that are typically associated with antiviral responses. Indicative of enhanced regulation to viral infection, we observed significantly dampened IFN responses in vMC<sub>0</sub>-infected neonates from OM-85-treated mothers when compared to those from untreated mothers, as evidenced by a reduction in both *IFN-β* (Figure 4p) and *IFN-γ* (Figure 4q) gene expression levels. Moreover, neonates of mothers exposed to gestational OM-85 treatment additionally displayed a heightened type 2-associated *IL-5* gene response when compared to those from untreated mothers (Figure 4r).

## DISCUSSION

Acute LRIs are the leading cause of death among children below the age of 5 years, with risk being highest in the neonatal/infancy period that precedes completion of the postnatal development process leading to establishment of immune competence. In the animal model studies presented here, we tested the hypothesis that mitigation of this risk may be achievable by stimulation of precocious postnatal maturation of immune competence via maternal treatment with a bacteria-derived immune training agent (OM-85) during pregnancy. To achieve this, we developed a neonatal model of vMC<sub>0</sub>-induced LRI, which accurately recapitulates the enhanced susceptibility to severe respiratory viral infection morbidity/mortality during early life. As a proof of concept, our data demonstrate that maternal OM-85 treatment during pregnancy mediates transplacental effects that significantly enhance resistance of their neonates to an otherwise lethal respiratory viral infection with the HRV-mimic vMC<sub>0</sub>. This protection was associated with significant attenuation of viral load within the lungs, and for the first time, we demonstrate parallel reduction in viral load within the brain of vMC<sub>0</sub>-infected neonates, findings consistent with

previous infection-related studies examining the effects of oral OM-85 treatment in adult mice.<sup>29,42</sup> It is pertinent to note in this regard that virus-related acute encephalopathy is one of the leading complications associated with virus-induced mortality in children.<sup>49,50</sup> At the cellular level, we demonstrate significant attenuation of the acute innate response within the peripheral lungs of vMC<sub>0</sub>-infected neonates from OM-85-treated mothers. Moreover, maternal OM-85 treatment enhanced the early postnatal expression of key function-associated molecules (MHC class II and CD86) on airway DC subsets within vMC<sub>0</sub>-infected neonates, again paralleling our previous reports in an experimental model of allergic airway inflammation.<sup>31</sup> This cellular response was accompanied by concomitant attenuation of the intensity of *IFN* gene expression profiles in vMC<sub>0</sub>-infected neonatal lungs at the peak of disease, while boosting type 2-associated *IL-5* gene expression.

Aberrant activation of innate antiviral pathways during the neonatal/infant period, owing largely to development-associated deficiencies in immune regulatory networks,<sup>14,15</sup> can facilitate collateral tissue damage within the lungs, with the most severe perturbations potentially life-threatening.<sup>11–13</sup> Here, we demonstrate the capacity for maternal OM-85 treatment during pregnancy to transplacentally regulate the intensity of vMC<sub>0</sub>-induced *IFN* responses in the lungs of their neonatal offspring. Moreover, the dampening of *IFN-γ* during murine respiratory viral infection has been reported to enhance ILC2 function in the lungs<sup>51</sup>, which, in conjunction with the upregulated subset of cells displaying an ILC2-like phenotype at DPI 5, provides a possible explanation as to the cellular source of enhanced *IL-5* gene expression within the lungs of vMC<sub>0</sub>-infected neonates from OM-85-treated mothers, given their capacity to produce greater amounts of *IL-5* than CD4<sup>+</sup> T cells on a per-cell basis following antigenic stimulation.<sup>52</sup> In further association with this apparent T-cell signature, vMC<sub>0</sub>-infected offspring from OM-85-treated mothers display an enhanced pool of Treg within the lungs. Collectively, these results mirror major findings from earlier studies on the mechanism of action of OM-85, namely (i) protection of maternal gestational challenge against the toxic effects of bacterial challenge via OM-85-mediated targeting of proinflammatory *IFN-γ* gene networks,<sup>29</sup> (ii) enhanced T-cell activation-

associated signatures in foetal bone marrow following maternal OM-85 treatment during pregnancy<sup>30</sup> and (iii) oral OM-85-mediated boosting of airway Treg pools in response to local inflammatory challenge.<sup>31,38,48</sup> Furthermore, these findings parallel independent studies demonstrating a role for Treg in the clearance of respiratory virus in neonatal mice.<sup>53</sup>

Insight into the nature of OM-85-induced transplacental mechanisms promoting offspring protection to respiratory viral infection was provided in the offspring of OM-85-treated mothers in the absence of neonatal vMC<sub>0</sub> infection, whose lungs displayed an enriched baseline pool of cDC subsets as evidenced by their increased numbers and maturation/activation states. In this regard, immunoregulatory DC networks in the early postnatal airway mucosa are typically developmentally compromised in both humans<sup>19,20</sup> and experimental animals<sup>21–23</sup> in regard to both population density and functional maturity. These findings mirror our previous discovery of accelerated postnatal establishment of functionally mature DC networks in respiratory tissues of offspring from OM-85-treated mothers.<sup>31</sup> Furthermore, we have previously identified the capacity of OM-85 to act transplacentally to expand the foetal bone marrow myeloid progenitor compartment by late gestation,<sup>30</sup> which ultimately gives rise to the broad repertoire of DC responsible for seeding the lungs during postnatal immunological development. Concomitant with the enhanced innate myeloid response, maternal OM-85 treatment additionally enriched the baseline pool of lung Tregs in neonates at 7 days of age, further supporting a role for transplacental OM-85 treatment in the accelerated establishment of a basal regulatory state in neonatal lungs.

Studies performed by our research team<sup>30</sup> have previously identified analogous hallmark immune training signatures shared between OM-85 treatment and the classical training agents  $\beta$ -glucan and BCG.<sup>54–56</sup> In the data presented here, we further expand on these shared features by identifying additional parallel mechanisms in the form of upregulated IL-1 $\beta$  and NLRP3 inflammasome complex.<sup>54,57</sup> It is pertinent to note in this regard that activation of endoplasmic reticulum unfolded protein response pathways, a recognised transplacental mechanism of maternal OM-85-mediated immune training within foetal bone marrow,<sup>30</sup> is associated with modulation of

the NLRP3 inflammasome complex<sup>58</sup> and DC function and survival,<sup>59</sup> particularly within the lungs.<sup>60</sup> Together with the pleotropic role of IL-1 $\beta$  in promoting proliferation and differentiation of myeloid progenitors,<sup>54,61</sup> these data suggest maternal OM-85 treatment transplacentally fosters a tissue microenvironment within the neonatal offspring lungs tailored towards myelopoiesis in the absence of inflammatory perturbation. Moreover, the dual NLRP3/caspase-1 signal required for IL-1 $\beta$  expression is only observed within baseline offspring lungs at PND 22 following maternal OM-85 treatment, paralleling previous studies revealing that OM-85 acts as a priming signal for the NLRP3 inflammasome complex,<sup>62</sup> known to be functionally compromised during prenatal and neonatal development,<sup>16,17</sup> and suggests that optimisation of the peripheral lung myeloid network is maintained throughout later life. However, given that IL-1 $\beta$  has primarily been investigated by others for its antiviral properties, a process dependent on stimulation of NLRP3/caspase-1,<sup>63–65</sup> further investigation of the role of this inflammasome pathway in the downstream protection against lethal severe LRI is warranted. Nevertheless, we have now established that OM-85-mediated upregulation of offspring myelopoiesis occurs from *in utero* development into adolescence,<sup>30,31</sup> thereby demonstrating that multiple mechanisms, operating over distinct time scales, may be responsible for this enhanced functional immunocompetence.

In this regard, a crucial mechanistic finding within the study presented here is the enhanced TLR expression in neonatal peripheral lung following maternal OM-85 treatment. Differentiation of myeloid cells is dependent on signalling via TLRs,<sup>66–68</sup> with impaired TLR signalling during early-life development in part responsible for the functional immaturity of the myeloid network within neonates.<sup>18</sup> Moreover, levels of TLR expression are recognised as key determinants of responsiveness to environmental microbial stimuli exemplified by farm dust, which are known to promote development of resistance to early asthma onset in both humans<sup>34,35,69</sup> and murine models.<sup>37</sup> Specific to respiratory viral infection, pre-exposure of human primary bronchial epithelial cells to farm dust extract significantly enhances TLR2 expression and limits HRV viral load in a TLR2/barrier function-dependent manner,<sup>36</sup> while neonatal murine TLR4 stimulation prior to severe RSV infection promotes

the generation of an 'adult-like' antiviral response, associated with an increase in cDC activation within the airways,<sup>70</sup> mirroring features of the data presented here. Taken together, we therefore postulate that optimisation of innate microbial sensing machinery via enhanced TLR4 and TLR7 expression within neonatal peripheral lungs is one of the primary maternal OM-85-mediated mechanisms promoting upregulation of myeloid subsets and accelerated functional immunocompetence of the neonatal respiratory myeloid network. Furthermore, we have previously identified the maternal OM-85-mediated modulation of microRNAs associated with TLR4 expression within foetal bone marrow,<sup>30</sup> signifying that the enhanced offspring peripheral lung response may be a direct result of immune training events initiated *in utero*.

We acknowledge several inherent limitations in this study, which need to be addressed in follow-up investigations. Firstly, we have no information on the cellular/transcriptomic response occurring between DPI 1 and 5, and such data may provide valuable insight into which neonates would ultimately succumb to viral infection and which would be protected, given the transient nature of the innate viral response following acute vMC<sub>0</sub> infection.<sup>7,71</sup> Secondly, we are unable to make precise distinctions between the roles of immune/inflammatory cell populations, which have extravasated into peripheral lung tissues and corresponding marginal pools adherent to vessel walls, given the inability to efficiently perfuse fragile neonatal lungs prior to tissue harvest. In this regard, it is known that the marginated pool of lung immune/inflammatory cells, particularly neutrophils,<sup>8,72</sup> is primed to rapidly extravasate from the lung vasculature and thus represents a crucial component of the acute innate response to inflammatory stimuli, and the lung-associated peripheral T-cell compartment is similarly partitioned<sup>73,74</sup>; this particular limitation is thus common to almost all studies in this area. Lastly, we have not identified the cellular source within lung tissue of enhanced TLR expression in the offspring of OM-85-treated mothers. In this regard, mesenchymal and epithelial cells within the lungs are known to express a broad repertoire of TLRs crucial in dictating function during immune responses.<sup>75,76</sup> Moreover, the process of trained immunity has recently been extended beyond haematopoietic immune cells.<sup>36,77</sup> The potential solution to these issues in

the future may be to employ a combination of cell sorting/single-cell RNA sequencing to enable high-precision mapping of the innate response on a per-cell basis in different lung tissue compartments. Notwithstanding these limitations, the strength of the protective effects of OM-85 in this model against respiratory pathogen challenge in the uniquely susceptible neonatal/infant age group provides strong justification for progression towards translational studies in human pregnancy.

## METHODS

### Animals

Specific pathogen-free BALB/c mice were purchased from the Animal Resource Centre (Murdoch). All mice were housed under specific pathogen-free conditions with standard food and water *ad libitum* at the Telethon Kids Institute Bioresources Centre.

### Time-mated pregnancies

Female BALB/c mice aged 8–12 weeks were time-mated with male BALB/c studs aged 8–26 weeks. Male studs were individually housed with 1–2 females overnight. The detection of a vaginal plug the following morning was designated gestation day (GD) 0.5.

### Maternal OM-85 treatment regimen

OM-85 (OM Pharma, Switzerland) is an endotoxin-low lyophilised standardised extract containing multiple TLR ligands derived from 8 major common respiratory bacterial pathogens (*Haemophilus influenzae*, *Streptococcus pneumoniae*, *Streptococcus pyogenes*, *Streptococcus viridians*, *Klebsiella pneumoniae*, *Klebsiella ozaenae*, *Staphylococcus aureus* and *Neisseria catarrhalis*).<sup>78</sup> Based on previously optimised pre-clinical dosing concentrations in pregnant mice,<sup>29,31</sup> time-mated pregnant BALB/c mice received daily oral feeding of lyophilised OM-85 reconstituted in phosphate-buffered saline (PBS) at a concentration of 400 mg kg<sup>-1</sup> (17.5% active pharmaceutical ingredient) body weight from GD0.5–17.5. Control pregnant mice were left untreated for the duration of the study. All maternal treatment was performed with a single batch of OM-85 (batch# 1812162).

### Neonatal Mengovirus (vMC<sub>0</sub>) infection

Attenuated mengovirus (vMC<sub>0</sub>) was prepared as previously described.<sup>7</sup> Two-day-old BALB/c neonatal mice from OM-85-treated and untreated mothers were intranasally inoculated with 10  $\mu$ L of either 10<sup>3</sup>, 10<sup>4</sup>, 10<sup>5</sup> or 10<sup>6</sup> plaque-forming-units (PFU) of live attenuated vMC<sub>0</sub>. Following vMC<sub>0</sub> dose titrations, 10<sup>4</sup> PFU was used for all experimental inoculations.

## Tissue collection

Neonates were autopsied at day post-infection (DPI) 1, 5, 10 and 20, which equates to postnatal day (PND) 3, 7, 12 and 22. Pre-perfusion of lung tissues from neonatal/infant animals was not feasible because of tissue fragility and so we standardised throughout to collection of samples from non-perfused lungs, which hence included marginating immune/inflammatory cell populations present on endothelial surfaces of the lung vascular bed,<sup>8,72–74,79–81</sup> plus a small contribution from occluded blood. Peripheral lung and brain tissue were collected and stored in either cold PBS + 0.1% bovine serum albumin (BSA; Bovogen Biologicals, Melbourne) for flow cytometric analysis, or RNeasy Stabilization Solution (Sigma-Aldrich, St. Louis) for analysis of gene expression profiles and viral titres. Samples collected into RNeasy Stabilization Solution were stored overnight at 4°C, then transferred to 1.5-mL Eppendorf tubes (Eppendorf) and frozen at –80°C for future analysis.

## Single-cell suspension preparation

Neonatal lungs were prepared by enzymatic digestion as previously described.<sup>31</sup> Briefly, lungs were minced with a scalpel and resuspended in 10 mL GKN + 10% foetal calf serum (FCS; Serana, Bunbury) with collagenase IV (Worthington Biochemical Corporation; Lakewood) and DNase (Sigma-Aldrich; St. Louis) at 37°C under gentle agitation for 60 min. Digested cells were filtered through sterile nylon, centrifuged and resuspended in cold PBS for total cell counts.

## Flow cytometry

Neonatal lung single-cell suspensions were used for all immunostaining. Panels of monoclonal antibodies (purchased from BD Bioscience unless otherwise stated) were developed to enable phenotypic characterisation of leucocytes of myeloid: CD45-PerCP (clone 30-F11), CD11b-v500 (clone M1/70), CD11c-AF700 (clone HL3), CD19-BV786 (clone 1D3), CD103-PE (clone M290), CD301-PE-Cy7 (clone MGL1/MGL2; BioLegend), F4/80-FITC (clone BM8; BioLegend, San Diego), Ly6G/C-APC-Cy7 (clone RB6-8C5), I-A/I-E-AF647 (clone M5/114.14.2) and B220/CD45R-PE-CF594 (clone RA3-6B2) and lymphoid: CD45-PerCP (clone 30-F11), NKp46-PE-Cy7 (clone 29A1.4; BioLegend), CD19-BV786 (clone 1D3), CD3-FITC (clone 17A2), CD4-v500 (clone RM4-5), CD8 $\alpha$ -BV650 (clone 53-6.7), CD25-APC-Cy7 (clone PC61) and Foxp3-PE (clone FJK-16s) lineages. Intracellular staining for Foxp3 was performed using an intracellular Foxp3/Transcription Factor Staining Buffer Kit (eBioscience, San Diego). All samples were kept as individuals. Immune cell phenotypic characterisation was performed using the FlowJo software (version 10.6.1; BD Bioscience). Fluorescent minus one staining controls were used for all panels where necessary. Flow cytometry data quality was based on primary time gates to ensure appropriate laser delay (pre-determined by automated CS&T) during sample acquisition.

## Viral titre

vMC<sub>0</sub> viral titre was measured in lung and brain homogenates by real-time quantitative polymerase chain reaction (RT-qPCR). Lungs and brain were homogenised in PBS (10% w/v) using a rotor-star homogeniser (Qiagen, Hilden), and total RNA was extracted using TRIzol (Invitrogen, Waltham) and RNeasy MinElute Cleanup Kit (Qiagen, Hilden). Complementary DNA (cDNA) was prepared via QuantiTect Reverse Transcription Kit (Qiagen, Hilden) and vMC<sub>0</sub> viral copy-number determined using the QuantiFast SYBR Green PCR Kit (Qiagen, Hilden) via the primer sequence: *forward primer*: 5'-GCC GAAAGC CAC GTG TGT AA and *reverse primer*: 5'-AGA TCC CAG CCA GTG GGG TA.<sup>71</sup> Viral copy numbers were calculated using a standard curve of known amounts of amplified cDNA.

## Cytokine and cellular sensor analysis

Cytokines and cellular sensors were measured in neonatal lung homogenates (cDNA prepared as per viral titres) by RT-qPCR using QuantiFast SYBR Green PCR Kit (Qiagen, Hilden) and QuantiTect Primer Assays (Qiagen, Hilden; as per the manufacturer's instructions) for the detection of *IL-1 $\alpha$* , *IL-1 $\beta$* , *IL-5*, *IFN- $\beta$* , *IFN- $\gamma$* , *NLRP3*, *caspase-1*, *TLR4* and *TLR7*.

## Statistical analysis

Statistical analysis and graphing was performed using the GraphPad Prism (version 8.3.0; GraphPad Software). Statistical significance of  $P < 0.05$  was considered significant. Two-way analyses of variance (ANOVA) followed by uncorrected Fisher's LSD test or Tukey's multiple comparisons test and the log-rank (Mantel-Cox) test were used for analyses as outlined in corresponding figure legends.

## Study approval

All animal experiments were formally approved by the Telethon Kids Institute Animal Ethics Committee, which operates under guidelines developed by the National Health and Medical Research Council of Australia for the care and use of animals in scientific research.

## ACKNOWLEDGMENTS

The authors acknowledge the animal technicians at the Telethon Kids Institute Bioresources Centre. This study was funded by the Asthma Foundation of Western Australia and Telethon Kids Institute. JFLJ was supported by a fellowship from the Fond de Recherche du Québec en Santé.

## CONFLICT OF INTERESTS

All authors declare that no competing interests exist.

## AUTHOR CONTRIBUTIONS

**Jean-Francois Lauzon-Joset:** Conceptualization; Data curation; Formal analysis; Funding acquisition; Methodology; Project administration; Supervision; Visualization; Writing-original draft; Writing-review & editing. **Kyle T Mincham:** Data curation; Formal analysis; Investigation; Methodology; Visualization; Writing-original draft; Writing-review & editing. **Naomi M Scott:** Formal analysis; Methodology; Project administration; Supervision. **Yasmine Khandan:** Formal analysis; Investigation. **Philip A Stumbles:** Formal analysis; Writing-original draft; Writing-review & editing. **Patrick G Holt:** Formal analysis; Writing-original draft; Writing-review & editing. **Deborah H Strickland:** Conceptualization; Formal analysis; Funding acquisition; Methodology; Supervision; Writing-original draft; Writing-review & editing.

## REFERENCES

- Liu L, Oza S, Hogan D et al. Global, regional, and national causes of under-5 mortality in 2000–15: an updated systematic analysis with implications for the Sustainable Development Goals. *Lancet* 2016; **388**: 3027–3035.
- Troeger C, Blacker B, Khalil IA et al. Estimates of the global, regional, and national morbidity, mortality, and aetiologies of lower respiratory infections in 195 countries, 1990–2016: a systematic analysis for the Global Burden of Disease Study 2016. *Lancet Infect Dis* 2018; **18**: 1191–1210.
- Kusel MM, de Klerk NH, Kebadze T et al. Early-life respiratory viral infections, atopic sensitization, and risk of subsequent development of persistent asthma. *J Allergy Clin Immunol* 2007; **119**: 1105–1110.
- Jackson DJ, Gangnon RE, Evans MD et al. Wheezing rhinovirus illnesses in early life predict asthma development in high-risk children. *Am J Respir Crit Care Med* 2008; **178**: 667–672.
- Lemanske RF Jr, Jackson DJ, Gangnon RE et al. Rhinovirus illnesses during infancy predict subsequent childhood wheezing. *J Allergy Clin Immunol* 2005; **116**: 571–577.
- Gern JE, Vrtis R, Grindle KA, Swenson C, Busse WW. Relationship of upper and lower airway cytokines to outcome of experimental rhinovirus infection. *Am J Respir Crit Care Med* 2000; **162**: 2226–2231.
- Rosenthal LA, Szakaly RJ, Amineva SP et al. Lower respiratory tract infection induced by a genetically modified picornavirus in its natural murine host. *PLoS One* 2012; **7**: e32061.
- Juliana A, Zonneveld R, Plotz FB, van Meurs M, Wilschut J. Neutrophil-endothelial interactions in respiratory syncytial virus bronchiolitis: An understudied aspect with a potential for prediction of severity of disease. *J Clin Virol* 2020; **123**: 104258.
- Asselin-Paturel C, Trinchieri G. Production of type I interferons: plasmacytoid dendritic cells and beyond. *J Exp Med* 2005; **202**: 461–465.
- Biron CA, Brossay L. NK cells and NKT cells in innate defense against viral infections. *Curr Opin Immunol* 2001; **13**: 458–464.
- Gern JE. Rhinovirus and the initiation of asthma. *Curr Opin Allergy Clin Immunol* 2009; **9**: 73–78.
- Narasaraju T, Yang E, Samy RP et al. Excessive neutrophils and neutrophil extracellular traps contribute to acute lung injury of influenza pneumonia. *Am J Pathol* 2011; **179**: 199–210.
- Everard ML, Swarbrick A, Wraitham M et al. Analysis of cells obtained by bronchial lavage of infants with respiratory syncytial virus infection. *Arch Dis Child* 1994; **71**: 428–432.
- Jones AC, Anderson D, Galbraith S et al. Personalized transcriptomics reveals heterogeneous immunophenotypes in children with viral bronchiolitis. *Am J Respir Crit Care Med* 2019; **199**: 1537–1549.
- Jones AC, Anderson D, Galbraith S et al. Immunoinflammatory responses to febrile lower respiratory infections in infants display uniquely complex/intense transcriptomic profiles. *J Allergy Clin Immunol* 2019; **144**: 1411–1413.
- Sharma AA, Jen R, Kan B et al. Impaired NLRP3 inflammasome activity during fetal development regulates IL-1 $\beta$  production in human monocytes. *Eur J Immunol* 2015; **45**: 238–249.
- Philbin VJ, Dowling DJ, Gallington LC et al. Imidazoquinoline Toll-like receptor 8 agonists activate human newborn monocytes and dendritic cells through adenosine-refractory and caspase-1-dependent pathways. *J Allergy Clin Immunol* 2012; **130**: 195–204 e199.
- Levy O, Zarembek KA, Roy RM, Cywes C, Godowski PJ, Wessels MR. Selective impairment of TLR-mediated innate immunity in human newborns: neonatal blood plasma reduces monocyte TNF- $\alpha$  induction by bacterial lipopeptides, lipopolysaccharide, and imiquimod, but preserves the response to R-848. *J Immunol* 2004; **173**: 4627–4634.
- Tschernig T, Debertin AS, Paulsen F, Kleemann WJ, Pabst R. Dendritic cells in the mucosa of the human trachea are not regularly found in the first year of life. *Thorax* 2001; **56**: 427–431.
- Heier I, Malmstrom K, Sajantila A, Lohi J, Makela M, Jahnsen FL. Characterisation of bronchus-associated lymphoid tissue and antigen-presenting cells in central airway mucosa of children. *Thorax* 2011; **66**: 151–156.
- Nelson DJ, McMenamin C, McWilliam AS, Brennan M, Holt PG. Development of the airway intraepithelial dendritic cell network in the rat from class II major histocompatibility (Ia)-negative precursors: differential regulation of Ia expression at different levels of the respiratory tract. *J Exp Med* 1994; **179**: 203–212.
- Nelson DJ, Holt PG. Defective regional immunity in the respiratory tract of neonates is attributable to hyporesponsiveness of local dendritic cells to activation signals. *J Immunol* 1995; **155**: 3517–3524.
- Ruckwardt TJ, Malloy AM, Morabito KM, Graham BS. Quantitative and qualitative deficits in neonatal lung-migratory dendritic cells impact the generation of the CD8<sup>+</sup> T cell response. *PLoS Pathog* 2014; **10**: e1003934.
- Holt PG, Strickland DH, Custovic A. Targeting maternal immune function during pregnancy for asthma prevention in offspring: Harnessing the "farm effect"? *J Allergy Clin Immunol* 2020; **146**: 270–272.

25. Schaad UB, Mütterlein R, Goffin H, Group BV-CS. Immunostimulation with OM-85 in children with recurrent infections of the upper respiratory tract: a double-blind, placebo-controlled multicenter study. *Chest* 2002; **122**: 2042–2049.
26. Razi CH, Harmanci K, Abaci A *et al.* The immunostimulant OM-85 BV prevents wheezing attacks in preschool children. *J Allergy Clin Immunol* 2010; **126**: 763–769.
27. Schaad UB. OM-85 BV, an immunostimulant in pediatric recurrent respiratory tract infections: a systematic review. *World J Pediatr* 2010; **6**: 5–12.
28. Esposito S, Bianchini S, Bosis S *et al.* A randomized, placebo-controlled, double-blinded, single-centre, phase IV trial to assess the efficacy and safety of OM-85 in children suffering from recurrent respiratory tract infections. *J Transl Med* 2019; **17**: 284.
29. Scott NM, Lauzon-Joset JF, Jones AC *et al.* Protection against maternal infection-associated fetal growth restriction: proof-of-concept with a microbial-derived immunomodulator. *Mucosal Immunol* 2017; **10**: 789–801.
30. Mincham KT, Jones AC, Bodinier M *et al.* Transplacental Innate Immune Training via Maternal Microbial Exposure: Role of XBP1-ERN1 Axis in Dendritic Cell Precursor Programming. *Front Immunol* 2020; **11**: 601494.
31. Mincham KT, Scott NM, Lauzon-Joset JF *et al.* Transplacental immune modulation with a bacterial-derived agent protects against allergic airway inflammation. *J Clin Invest* 2018; **128**: 4856–4869.
32. He YM, Li X, Perego M *et al.* Transitory presence of myeloid-derived suppressor cells in neonates is critical for control of inflammation. *Nat Med* 2018; **24**: 224–231.
33. Luan H, Zhang Q, Wang L *et al.* OM85-BV induced the productions of IL-1 $\beta$ , IL-6, and TNF- $\alpha$  via TLR4- and TLR2-mediated ERK1/2/NF- $\kappa$ B pathway in RAW264.7 cells. *J Interferon Cytokine Res* 2014; **34**: 526–536.
34. Lauener RP, Birchler T, Adamski J *et al.* Expression of CD14 and Toll-like receptor 2 in farmers' and nonfarmers' children. *Lancet* 2002; **360**: 465–466.
35. Ege MJ, Bieli C, Frei R *et al.* Prenatal farm exposure is related to the expression of receptors of the innate immunity and to atopic sensitization in school-age children. *J Allergy Clin Immunol* 2006; **117**: 817–823.
36. van der Vlugt L, Eger K, Muller C *et al.* Farm dust reduces viral load in human bronchial epithelial cells by increasing barrier function and antiviral responses. *J Allergy Clin Immunol* 2018; **141**: 1949–1952 e1948.
37. Conrad ML, Ferstl R, Teich R *et al.* Maternal TLR signaling is required for prenatal asthma protection by the nonpathogenic microbe *Acinetobacter lwoffii* F78. *J Exp Med* 2009; **206**: 2869–2877.
38. Navarro S, Cossalter G, Chiavaroli C *et al.* The oral administration of bacterial extracts prevents asthma via the recruitment of regulatory T cells to the airways. *Mucosal Immunol* 2011; **4**: 53–65.
39. Yasui H, Kiyoshima J, Hori T. Reduction of influenza virus titer and protection against influenza virus infection in infant mice fed *Lactobacillus casei* Shirota. *Clin Diagn Lab Immunol* 2004; **11**: 675–679.
40. Culley FJ, Pollott J, Openshaw PJ. Age at first viral infection determines the pattern of T cell-mediated disease during reinfection in adulthood. *J Exp Med* 2002; **196**: 1381–1386.
41. Kumova OK, Fike AJ, Thayer JL *et al.* Lung transcriptional unresponsiveness and loss of early influenza virus control in infected neonates is prevented by intranasal *Lactobacillus rhamnosus* GG. *PLoS Pathog* 2019; **15**: e1008072.
42. Pasquali C, Salami O, Taneja M *et al.* Enhanced mucosal antibody production and protection against respiratory infections following an orally administered bacterial extract. *Front Med* 2014; **1**: 41.
43. Ng SL, Teo YJ, Setiagani YA, Karjalainen K, Ruedl C. Type 1 Conventional CD103<sup>+</sup> Dendritic Cells Control Effector CD8<sup>+</sup> T Cell Migration, Survival, and Memory Responses During Influenza Infection. *Front Immunol* 2018; **9**: 3043.
44. McWilliam AS, Nelson D, Thomas JA, Holt PG. Rapid dendritic cell recruitment is a hallmark of the acute inflammatory response at mucosal surfaces. *J Exp Med* 1994; **179**: 1331–1336.
45. Kim TS, Braciale TJ. Respiratory dendritic cell subsets differ in their capacity to support the induction of virus-specific cytotoxic CD8<sup>+</sup> T cell responses. *PLoS One* 2009; **4**: e4204.
46. Legge KL, Braciale TJ. Accelerated migration of respiratory dendritic cells to the regional lymph nodes is limited to the early phase of pulmonary infection. *Immunity* 2003; **18**: 265–277.
47. Strickland DH, Fear V, Shenton S *et al.* Persistent and compartmentalised disruption of dendritic cell subpopulations in the Lung following influenza A virus infection. *PLoS One* 2014; **9**: e111520.
48. Strickland DH, Judd S, Thomas JA, Larcombe AN, Sly PD, Holt PG. Boosting airway T-regulatory cells by gastrointestinal stimulation as a strategy for asthma control. *Mucosal Immunol* 2011; **4**: 43–52.
49. Britton PN, Dale RC, Blyth CC *et al.* Influenza-associated encephalitis/encephalopathy identified by the Australian childhood encephalitis study 2013–2015. *Pediatr Infect Dis J* 2017; **36**: 1021–1026.
50. Okuno H, Yahata Y, Tanaka-Taya K *et al.* Characteristics and outcomes of influenza-associated encephalopathy cases among children and adults in Japan, 2010–2015. *Clin Infect Dis* 2018; **66**: 1831–1837.
51. Califano D, Furuya Y, Roberts S, Avram D, McKenzie ANJ, Metzger DW. IFN- $\gamma$  increases susceptibility to influenza A infection through suppression of group II innate lymphoid cells. *Mucosal Immunol* 2018; **11**: 209–219.
52. Patel DF, Peiro T, Bruno N *et al.* Neutrophils restrain allergic airway inflammation by limiting ILC2 function and monocyte-dendritic cell antigen presentation. *Sci Immunol* 2019; **4**: eaax7006.
53. Oliphant S, Lines JL, Hollifield ML, Garvy BA. Regulatory T cells are critical for clearing influenza A virus in neonatal mice. *Viral Immunol* 2015; **28**: 580–589.
54. Mitroulis I, Ruppova K, Wang B *et al.* Modulation of myelopoiesis progenitors is an integral component of trained immunity. *Cell* 2018; **172**: 147–161 e112.
55. Moorlag S, Khan N, Novakovic B *et al.*  $\beta$ -glucan induces protective trained immunity against *Mycobacterium tuberculosis* infection: a key role for IL-1. *Cell Rep* 2020; **31**: 107634.

56. Kaufmann E, Sanz J, Dunn JL *et al.* BCG educates hematopoietic stem cells to generate protective innate immunity against tuberculosis. *Cell* 2018; **172**: 176–190 e119.
57. Christ A, Gunther P, Lauterbach MAR *et al.* Western diet triggers NLRP3-dependent innate immune reprogramming. *Cell* 2018; **172**: 162–175 e114.
58. Chong WC, Shastri MD, Peterson GM *et al.* The complex interplay between endoplasmic reticulum stress and the NLRP3 inflammasome: a potential therapeutic target for inflammatory disorders. *Clin Transl Immunology* 2021; **10**: e1247.
59. Iwakoshi NN, Pypaert M, Glimcher LH. The transcription factor XBP-1 is essential for the development and survival of dendritic cells. *J Exp Med* 2007; **204**: 2267–2275.
60. Tavernier SJ, Osorio F, Vandersarren L *et al.* Regulated IRE1-dependent mRNA decay sets the threshold for dendritic cell survival. *Nat Cell Biol* 2017; **19**: 698–710.
61. Pietras EM, Mirantes-Barbeito C, Fong S *et al.* Chronic interleukin-1 exposure drives haematopoietic stem cells towards precocious myeloid differentiation at the expense of self-renewal. *Nat Cell Biol* 2016; **18**: 607–618.
62. Dang AT, Pasquali C, Ludigs K, Guarda G. OM-85 is an immunomodulator of interferon- $\beta$  production and inflammasome activity. *Sci Rep* 2017; **7**: 43844.
63. Peiro T, Patel DF, Akthar S *et al.* Neutrophils drive alveolar macrophage IL-1 $\beta$  release during respiratory viral infection. *Thorax* 2018; **73**: 546–556.
64. Thomas PG, Dash P, Aldridge JR Jr *et al.* The intracellular sensor NLRP3 mediates key innate and healing responses to influenza A virus via the regulation of caspase-1. *Immunity* 2009; **30**: 566–575.
65. Allen IC, Scull MA, Moore CB *et al.* The NLRP3 inflammasome mediates in vivo innate immunity to influenza A virus through recognition of viral RNA. *Immunity* 2009; **30**: 556–565.
66. Krutzik SR, Tan B, Li H *et al.* TLR activation triggers the rapid differentiation of monocytes into macrophages and dendritic cells. *Nat Med* 2005; **11**: 653–660.
67. Nagai Y, Garrett KP, Ohta S *et al.* Toll-like receptors on hematopoietic progenitor cells stimulate innate immune system replenishment. *Immunity* 2006; **24**: 801–812.
68. Megias J, Yanez A, Moriano S, O'Connor JE, Gozalbo D, Gil ML. Direct Toll-like receptor-mediated stimulation of hematopoietic stem and progenitor cells occurs in vivo and promotes differentiation toward macrophages. *Stem Cells* 2012; **30**: 1486–1495.
69. Eder W, Klimecki W, Yu L *et al.* Toll-like receptor 2 as a major gene for asthma in children of European farmers. *J Allergy Clin Immunol* 2004; **113**: 482–488.
70. Malloy AM, Ruckwardt TJ, Morabito KM, Lau-Kilby AW, Graham BS. Pulmonary dendritic cell subsets shape the respiratory syncytial virus-specific CD8<sup>+</sup> T cell immunodominance hierarchy in neonates. *J Immunol* 2017; **198**: 394–403.
71. Lauzon-Joset JF, Jones AC, Mincham KT *et al.* Atopy-dependent and independent immune responses in the heightened severity of atopics to respiratory viral infections: rat model studies. *Front Immunol* 2018; **9**: 1805.
72. Kreisel D, Nava RG, Li W *et al.* In vivo two-photon imaging reveals monocyte-dependent neutrophil extravasation during pulmonary inflammation. *Proc Natl Acad Sci USA* 2010; **107**: 18073–18078.
73. Pabst R, Binns RM, Licence ST, Peter M. Evidence of a selective major vascular marginal pool of lymphocytes in the lung. *Am Rev Respir Dis* 1987; **136**: 1213–1218.
74. Nelson D, Strickland D, Holt PG. Selective attrition of non-recirculating T cells during normal passage through the lung vascular bed. *Immunology* 1990; **69**: 476–481.
75. Pevsner-Fischer M, Morad V, Cohen-Sfady M *et al.* Toll-like receptors and their ligands control mesenchymal stem cell functions. *Blood* 2007; **109**: 1422–1432.
76. Sveiven SN, Nordgren TM. Lung-resident mesenchymal stromal cells are tissue-specific regulators of lung homeostasis. *Am J Physiol Lung Cell Mol Physiol* 2020; **319**: L197–L210.
77. Naik S, Larsen SB, Gomez NC *et al.* Inflammatory memory sensitizes skin epithelial stem cells to tissue damage. *Nature* 2017; **550**: 475–480.
78. Rozy A, Chorostowska-Wynimko J. Bacterial immunostimulants—mechanism of action and clinical application in respiratory diseases. *Pneumonol Alergol Pol* 2008; **76**: 353–359.
79. Holt PG, Degebrodt A, Venaille T *et al.* Preparation of interstitial lung cells by enzymatic digestion of tissue slices: preliminary characterization by morphology and performance in functional assays. *Immunology* 1985; **54**: 139–147.
80. Doerschuk CM, Allard MF, Martin BA, MacKenzie A, Autor AP, Hogg JC. Marginated pool of neutrophils in rabbit lungs. *J Appl Physiol (1985)* 1987; **63**: 1806–1815.
81. Lien DC, Wagner WW Jr, Capen RL *et al.* Physiological neutrophil sequestration in the lung: visual evidence for localization in capillaries. *J Appl Physiol (1985)* 1987; **62**: 1236–1243.

## Supporting Information

Additional supporting information may be found online in the Supporting Information section at the end of the article.



This is an open access article under the terms of the Creative Commons Attribution-NonCommercial-NoDerivs License, which permits use and distribution in any medium, provided the original work is properly cited, the use is non-commercial and no modifications or adaptations are made.